'91 韓國自動制御學術會議論文集 1991. 10.22~24

Energy Constraint Control in Numerical Simulation of Constrained Dynamic Systems

선임연구원 윤 석 준

대한항공 항공기술연구원

S. Yoon

Korea Institute of Aeronautical Technology, Seoul, Korea

Abstract

In the analysis of constrained holonomic systems, the Lagrange multiplier method yields a system of second-order ordinary differential equations of motion and algebraic constraint equations. Conventional holonomic or nonholonomic constraints are defined as geometric constraints in this paper. Previous works concentrate on the geometric constraints. However, if the total energy of a dynamic system can be computed from the initial energy plus the time integral of the energy input rate due to external or internal forces, then the total energy can be artificially treated as a constraint. The violation of the total energy constraint due to numerical errors can be used as information to control these errors. It is a necessary condition for accurate simulation that both geometric and energy constraints be satisfied. When geometric constraint control is combined with energy constraint control, numerical simulation of a constrained dynamic system becomes more accurate. A new convenient and effective method to implement energy constraint control in numerical simulation is developed based on the geometric interpretation of the relation between constraints in the phase space. Several combinations of energy constraint control with either Baumgarte's Constraint Violation Stabilization Method (CVSM) are also addressed.

Introduction

In the analysis of constrained holonomic systems[1,2], the Lagrange multiplier method yields a system of second-order ordinary differential equations of motion and algebraic constraint equations. The Lagrange equations of motion, with the accompanying constraint equations for holonomic or nonholonomic systems, cannot in general be solved analytically.

Theoretical analyses[3-6] for general Lagrange equations with algebraic constraint equations show that constraint equations should be differentiated twice, in general, for the system to be solved numerically without iteration. The differentiation of constraint equations was suggested[7] prior to these analyses and was shown to result in unstable numerical solutions. The original constraint equations are rapidly violated, since the differentiated constraint equations are unstable and numerical errors during computation continuously disturb the system[8]. This problem was seemingly resolved by a modified form of second-order differential constraint equations. But this solution, the Constraint Violation Stabilization Method (CVSM)[9], did not work well for relatively complicated systems and had some ambiguity in determining optimal feedback gains.

Conventional holonomic or nonholonomic constraints are defined as geometric constraints in this paper. The aforementioned works concentrate on the geometric constraints. However, if the total energy of a dynamic system can be computed from the initial energy plus the time integral of the energy input rate due to external or internal forces, then the total energy can be artificially treated as a constraint. The violation of the total energy constraint due to numerical errors can be used as information to control these errors. It is a necessary condition for accurate simulation that both geometric and energy constraints be satisfied. When geometric constraint control is combined with energy constraint control, numerical simulation of a constrained dynamic system becomes more accurate.

First, constrained dynamic systems are introduced, using Lagrange multipliers, and then followed by the introduction of Baumgarte's Constraint Violation Stabilization Method (CVSM). Conventional methods for implementing energy constraint control are then reviewed. A new convenient and effective method to implement energy constraint control in numerical simulation is developed based on the geometric interpretation of the relation between constraints in the phase space.

Constrained Dynamic Systems

Constraints are either holonomic or nonholonomic. When the Lagrange multiplier method is applied to a dynamic system with holonomic constraints[1,2], the equations of motion are described by

$$M(q)\,\ddot{q} + \Phi_q^T\,\lambda = G(q,\dot{q},t) \qquad (1)$$

$$\Phi(q,t) = 0 \qquad (2)$$

where the holonomic constraint functions Φ: $R^{n+1} \rightarrow R^m$, generalized coordinates $q \in R^n$, $m < n$, and time $t \geq 0$. In Eq. (1), $\lambda \in R^m$ is a Lagrange multiplier. The inertia matrix $M \in R^{nxn}$ is positive definite, and $G \in R^n$ represents the remaining dynamic terms in the equation. Then the dynamic system with holonomic constraints is described by a set of n differential equations (1) and m algebraic equations (2).

If the Lagrange multiplier λ can be computed or expressed in terms of q, $\dot{q}$, and t, then the system of algebraic differential equations can be solved numerically. A fundamental method for computing λ without using implicit algorithms is to differentiate the constraint equation (2) twice with respect to time. This results in the equation

$$\ddot{\Phi}\,(q,\dot{q},\ddot{q},t) = 0 \qquad (3)$$

After some manipulations λ can be obtained in the form

$$\lambda = \Lambda(q,\dot{q},t) \qquad (4)$$

Eq. (4) is substituted back into (1) to yield

$$\ddot{q} = A\,(q,\dot{q},\Lambda(q,\dot{q},t),t) \qquad (5)$$

Since the n second-order differential equations in q do not involve the m Lagrange multipliers λ in (5), the equations of motion can be solved numerically. In this paper, Eq. (5) is the differential equation that forms the basis for the numerical simulations.

Baumgarte's Constraint Violation Stabilization Method

A control $U(\Phi,\dot{\Phi},t)$ can be added to the right side of Eq. (3) in order to stabilize the reduction of the geometric constraint violations. Thus we let

$$\ddot{\Phi} = U(\Phi,\dot{\Phi},t) \qquad (6)$$

where Baumgarte suggests the form

$$U \equiv -\alpha\dot{\Phi} - \beta\,\Phi \qquad (7)$$

The above arguments can be directly extended to nonholonomic constraints without any difficulty. In this case the constraint equation, modified to suppress the nonholonomic constraint violations, has the form

$$\dot{\Pi}(q,\dot{q},\ddot{q},t) = U(\Pi) = -\eta\,\Pi(q,\dot{q},t) \qquad (8)$$

where Π is a nonholonomic constraint function, and U is a control to stabilize the constraint violation. The nonholonomic constraint is differentiated only once, rather than twice as in the holonomic case, in order that the new equivalent system will be represented by second-order differential equations.

Energy Constraint Control Methods

There are at least two methods available in the literature for implementing an energy constraint, using the Lagrange equations of motion. The first method is described by Baumgarte[9]. The idea is to use the dynamic constraint equations modified from the original energy constraint equations in a manner similar to the nonholonomic case in Baumgarte's Constraint Violation stabilization Method (CVSM). If ψ is the energy constraint function, we let

$$\dot{\psi} + \eta\,\psi = 0, \qquad \psi = \psi(q,\dot{q}) \qquad (9)$$

In general,

$$\psi \equiv T + V - (T+V)_0 - \int_{t_0}^{t} \dot{E}\,d\tau$$

where $\dot{E}$ is the energy input rate to the system. For a conservative system

$$\psi = E - E_0$$

where E is the total energy, expressed in terms of q and $\dot{q}$. The Lagrange equation of motion for holonomic systems[8] can be described by

$$M(q)\,\ddot{q} + \Phi_q^T(q,t)\,\lambda = G(q,\dot{q},t)$$

If an energy constraint is added to the equation, then

$$M\,\ddot{q} + \Phi_q^T\,\lambda + \psi_{\dot{q}}^T\,\mu = G \qquad (10)$$

where λ and μ are Lagrange multipliers. After some manipulations we obtan

$$\mu = \left(\psi_{\dot{q}} M^{-1} \psi_q^T\right)^{-1} \left[\psi_{\dot{q}} M^{-1} \left(G - \Phi_q^T \lambda\right) + \psi_q \dot{q} + \eta \psi\right] \quad (11)$$

Substituting (11) back into (10) results in the equation of motion without μ, which is

$$\ddot{q} = M^{-1}\left(G - \Phi_q^T \lambda\right) \quad (12)$$

$$- M^{-1} \psi_q^T \left(\psi_{\dot{q}} M^{-1} \psi_q^T\right)^{-1} \left[\psi_{\dot{q}} M^{-1} \left(G - \Phi_q^T \lambda\right) + \psi_q \dot{q} + \eta \psi\right]$$

Here η should be chosen so that the energy constraint is stabilized.

The second method for implementing energy constraint control is based on the steepest descent algorithm[10]. The correction forces are applied to the equations of motion so that the integration of $\dot{q}$ and $\ddot{q}$ moves in the direction which most rapidly reduces the violation of the energy constraint[11]. To ensure that the minimum[12,13] of ψ is zero, the negative gradient of ψ^2 is fed back into the equations of motion (5). That is,

$$\frac{dq}{dt} = v - \rho_q \frac{\partial \psi^2}{\partial q} \quad (13)$$

$$\frac{dv}{dt} = A(q,v,t) - \rho_v \frac{\partial \psi^2}{\partial v}$$

Here ρ_q and ρ_v are positive gain constants to be determined and, ideally, $\psi(q,v) = 0$. Since $\partial\psi^2/\partial q = 2\psi(\partial\psi/\partial q)$ and $\partial\psi^2/\partial v = 2\psi(\partial\psi/\partial v)$, these control terms disappear when $\psi = 0$. In the analytic solution, $\psi = 0$ is satisfied. Thus, implementation of the energy constraint control in (13) does not change the exact solution of the original dynamic system equations. Both $\dot{q}$ and v can be considered to represent the total time derivative of q. However, d/dt is used to express the total time derivative when constraint control terms are added . The method in (13) of energy constraint control has been successfully applied in the computation of space and reentry trajectories[13]. Note that (13) is different from (12), and that (13) is simpler to implement.

A New Method of Implementing Energy Constraint Control

In the q, $\dot{q}$ phase space the surfaces of constant energy and the surfaces for conventional holonomic or nonholonomic constraints are not in general perpendicular to each other. The surfaces are given by

$\psi(q, \dot{q}) = 0$: Energy Constraint

$\chi_i(q, \dot{q}, t) = 0$, i=1,2,..., m : Geometric Constraints

In general,

$$\left\{\frac{\partial \psi}{\partial \begin{pmatrix} q \\ \dot{q} \end{pmatrix}}\right\} \left\{\frac{\partial \chi_i}{\partial \begin{pmatrix} q \\ \dot{q} \end{pmatrix}}\right\}^T \neq 0 \quad i=1,2,..., m \quad (14)$$

where $q, \dot{q} \in R^n$, $\psi : R^{2n} \rightarrow R$, and $\chi_i : R^{2n+1} \rightarrow R$. One case where the energy and geometric constraint surfaces are orthogonal is illustrated in the following example. Let

$$\psi(\dot{q})=0$$

and

$$\chi_i(q,t) = 0 \qquad i=1,2,...,m$$

Then

$$\left\{\frac{\partial \psi}{\partial \begin{pmatrix} q \\ \dot{q} \end{pmatrix}}\right\}^T = \begin{pmatrix} 0 \\ \frac{\partial \psi}{\partial \dot{q}} \end{pmatrix}$$

$$\left\{\frac{\partial \chi_i}{\partial \begin{pmatrix} q \\ \dot{q} \end{pmatrix}}\right\}^T = \begin{pmatrix} \frac{\partial \chi_i}{\partial q} \\ 0 \end{pmatrix}$$

Thus,

$$\left\{\frac{\partial \psi}{\partial \begin{pmatrix} q \\ \dot{q} \end{pmatrix}}\right\} \left\{\frac{\partial \chi_i}{\partial \begin{pmatrix} q \\ \dot{q} \end{pmatrix}}\right\}^T = 0 \quad (15)$$

The solution to the equations of motion of a given system can be interpreted as a point moving in the state-variable phase space. The necessary condition for the exact simulation of the given equations of motion is that the point moves along the common intersection of all the constraint surfaces in the phase space. Numerical errors in the simulation represent disturbances which continuously perturb the point from this common intersection. The constraint violation control is designed to minimize the effect of these disturbances and keep the point close to the constraint-surface intersection.

If violations of both geometric and energy constraints are relatively small, then the point is always close to the

constraint surface intersection. If a two-dimensional view is taken in the neighborhood of the intersection, then the lines indicating the constraints can be viewed as nearly linear, as in Fig 1. The intersection in the phase space is the origin O in this two-dimensional view, and the phase point is denoted as P in the figure. The point P is continually disturbed by the numerical integration errors during the simulation. The disturbance can be considered to be composed of two orthogonal components (d_{c_1},d_{c_2}) in the plane. When the CVSM is applied to control the geometric constraint violation, the CVSM forces the point P to move toward the $\chi_i = 0$ axis. Thus, the control of the CVSM generally has two components, (f_{c_1},f_{c_2}), where f_{c_1} is always directed toward the $\chi_i = 0$ axis. Note that the directions of d_{c_1},d_{c_2},and f_{c_2} may be reversed in the figure, and that the relative angle θ between two axes can be a function of the state variables and time, i.e., $\theta = \theta(q,\dot{q},t)$.

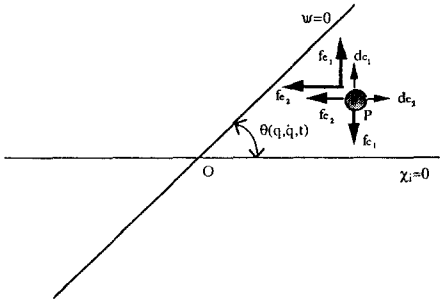

Fig 1. Two-dimensional geometric interpretation of CVSMs combined with energy constraint control in phase space.

If the constraint surfaces of the geometric and the energy constraints are not orthogonal to each other in the phase space, which in general will be the case, then the relative position of P with respect to the energy constraint surface is changed by applying geometric constraint control. There exists no guarantee that P moves toward the intersection O of the two constraint surfaces. In many cases P moves farther from the origin O when applying geometric constraint control alone. This phenomenon can be noted later in the test simulations. When strong geometric constraint control is applied to ensure very small geometric constraint errors, the resulting drift in the total energy can in many cases become very large. This in turn causes large errors in the state variables as functions of time. These arguments explain why a combination of geometric and energy constraint controls is essential for accurate simulation, i.e., to keep the point P close to the exact solution point O in Fig 1.

The conventional methods described in the previous section for implementing energy constraint control require the point to move toward the $\psi = 0$ axis. The control can be considered to be composed of two orthogonal components (f_{e_1},f_{e_2}), one perpendicular and one parallel to the $\chi_i = 0$ axis. The CVSM forces the point P to move toward the $\chi_i = 0$ axis while the energy control makes the point P move toward the $\psi = 0$ axis. Note again that the relative angle θ is a function of state variables and time, which makes the direction of the sum of (f_{e_1},f_{e_2}) difficult to predict. If the CVSM's are combined with conventional energy methods, the two different controls are geometrically coupled. That is, the control to make P move toward the origin O may not be simple.

A solution to this difficulty for the case of holonomic systems is to make the control of the energy constraint parallel to the geometric constraint. That is, in effect we have

$$\left\{\frac{\partial \psi}{\partial\begin{pmatrix} q \\ \dot{q}\end{pmatrix}}\right\}^T = \begin{Bmatrix} 0 \\ \dfrac{\partial \psi}{\partial \dot{q}} \end{Bmatrix} \tag{16}$$

by setting $\rho_q=0$. With $\rho_q=0$, Eq. (13) becomes

$$\frac{dq}{dt} = v$$
$$\frac{dv}{dt} \equiv A(q,v,t) - \rho_v \frac{\partial \psi^2}{\partial v} \tag{17}$$

Note that the geometric interpretation is not changed by replacing ψ by ψ^2. Replacement of ψ by ψ^2 makes the effect of the feedback control on the point P proportionally less as the point moves closer to the origin. That is,

$$\rho_v \frac{\partial \psi^2}{\partial v} = 2\rho_v \psi \frac{\partial \psi}{\partial v}$$

and the energy correction term in (17) varies linearly with ψ. By using (17) rather than (13), the control on the energy constraint becomes parallel to the geometric constraint, i.e., $f_{e_1} = 0$ and $\rho_q = 0$. Then

$$\left\{\frac{\partial \chi_i}{\partial\begin{pmatrix} q \\ \dot{q}\end{pmatrix}}\right\}^T = \begin{Bmatrix} \dfrac{\partial \chi_i}{\partial q} \\ 0 \end{Bmatrix} \tag{18}$$

and, from (16) and (18),

$$\left\{\frac{\partial \psi}{\partial \begin{pmatrix} q \\ \dot{q} \end{pmatrix}}\right\}\left\{\frac{\partial \chi_i}{\partial \begin{pmatrix} q \\ \dot{q} \end{pmatrix}}\right\}^T = 0 \quad i=1,2,\ldots,m \qquad (19)$$

Application of the control on the geometric constraint forces the point to move toward the geometric constraint. But it also changes the relative position of the point with respect to the energy constraint, since the two different surfaces are not perpendicular to each other. Because the control on the energy constraint is parallel to the geometric constraints, the energy control does not change the relative position of the point P with respect to the χ_i=0 axis. Thus the f_{e_1}component has been removed by setting ρ_q=0. Appropriate choice of the gains in (17) will force the point P to move toward the origin O despite the presence of truncation errors.

The difficulty associated with proper choice of these gains is dependent on how the constraints are coupled in phase space. The variable $Y_{ci}(q,\dot{q},t)$, defined as

$$\left\{\frac{\partial \psi}{\partial \begin{pmatrix} q \\ \dot{q} \end{pmatrix}}\right\}\left\{\frac{\partial \chi_i}{\partial \begin{pmatrix} q \\ \dot{q} \end{pmatrix}}\right\}^T \equiv Y_{ci}(q,\dot{q},t) \quad i=1,2,\ldots,m \qquad (20)$$

can be used as a measure of the degree of coupling when an energy constraint control and geometric constraint controls are combined. The larger the magnitude of Y_{ci}, the more substantial is the coupling.

Combination of Geometric Constraint Control and Energy Constraint Control

Baumgarte's CVSM in (7) with $U=-\alpha\dot{\Phi}-\beta\Phi$ leads to a set of equations of the form

$$\frac{dq}{dt} = v$$
$$\frac{dv}{dt} = A_B(q,v,t,\alpha,\beta) \qquad (21)$$

Note again that $\dot{q}$ is replaced by v and that $A_B = A$ if $\alpha = \beta = 0$. Both v and $\dot{q}$ represent the total time derivative of q. In this paper, d/dt is used to express the time derivative to be integrated numerically in the state equations. Combination of (13) and (21) results in

$$\frac{dq}{dt} = v - \rho_q \frac{\partial \psi^2}{\partial q}$$
$$\frac{dv}{dt} = A_B(q,v,t,\alpha,\beta) - \rho_v \frac{\partial \psi^2}{\partial v} \qquad (22)$$

If (17) is combined with (21), then

$$\frac{dq}{dt} = v$$
$$\frac{dv}{dt} = A_B(q,v,t,\alpha,\beta) - \rho_v \frac{\partial \psi^2}{\partial v} \qquad (23)$$

Note that the vector associated with $\partial\psi^2/\partial v$ in (23) is parallel to the Φ_i= 0 surface in the sense of satisfying (19) with $\Phi_i \equiv \chi_i$.

Test Simulations

It will be shown experimentally why control of geometric constraints only cannot yield accurate values of the state variables in the numerical simulation of constrained dynamic systems, even if the control may achieve successful suppression of the geometric constraint violations. The energy constraint control will trun out to be necessary for accurate simulation even when independent coordinates are chosen in the numerical simulation.

Example 1 (Fig 2)

A unit mass moves along a unit circle in the XY-plane. A gravity force Mg (M = 1) is applied in the negative Y-direction. This is just a simple pendulum problem, with the position of the unit pendulum mass with respect to the suspension point represented by the dependent rectangular coordinates X and Y rather than the usual independent polar coordinate θ. The pendulum length equals unity in the example. The equations of motion without constraint control are

$$\frac{d}{dt}X = V_X \qquad (24.a)$$

$$\frac{d}{dt}Y = V_Y \qquad (24.b)$$

$$\frac{d}{dt}V_X = -X\frac{V_X^2 + V_Y^2 - gY}{X^2 + Y^2} \qquad (24.c)$$

$$\frac{d}{dt}V_Y = -Y\frac{V_X^2 + V_Y^2 - gY}{X^2 + Y^2} \qquad (24.d)$$

The gravity g is fixed at 1 in the test simulations. In terms of rectangular coordinates X and Y the holonomic constraint equation is

$$\Phi = \frac{1}{2}(X^2 + Y^2 - 1) = 0 \qquad (25)$$

The energy constraint is

$$\psi = T + V - (T_0 + V_0)$$

$$= \frac{1}{2}\left(\dot{X}^2 + \dot{Y}^2\right) + gY - (T_0 + V_0) = 0 \qquad (26)$$

The initial conditions are

$$X(0)=1, \quad Y(0)=0, \quad \dot{X}(0)=0, \quad \dot{Y}(0)=2 \qquad (27)$$

With the initial conditions the pendulum starts with sufficient upward velocity to cause it to rotate continuously but with periodically-varying angular velocity. Accompanying time histories of the state variables are presented in Fig 3.

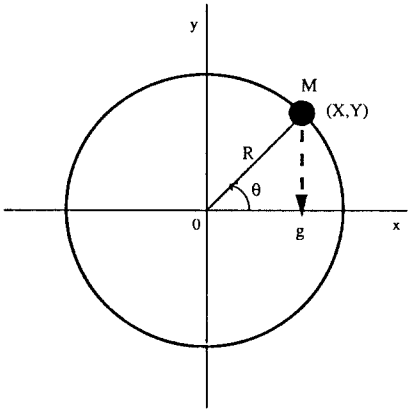

Fig 2. A unit mass rotating on a unit circle.

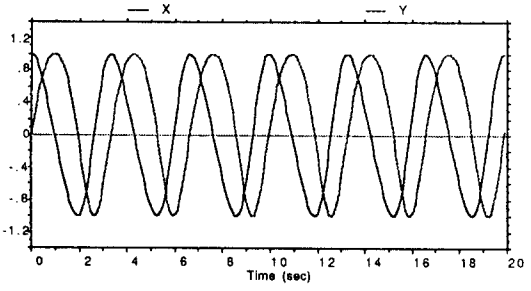

Fig 3. Example 1: Time histories of X and

Adams-Bashforth 3rd (AB-3) integration method is used with the integration step size h=0.01 sec in the test simulations. The start-up problem of AB-3 is resolved by using Runge-Kutta 4th-order (RK-4) integration to compute necessary initial start-up conditions. With this simple example six different cases are compared in geometric constraint violation Φ, energy constraint violation ψ, and time history of the errors in the state variable X. The case where no constraint controls are applied is shown in the Figs 4 through 6, as well as the case where Baumgarte's geometric constraint control is applied. In Baumgarte's CVSM critical damping is used for the gains α and β, i.e., $\beta = \alpha^2/4$, and $\beta = 40$ is chosen and integration step size h = 0.01. The other two cases compared in the figures use an independent coordinate by choosing θ as a state variable, where θ is a counterclockwise angular displacement of the unit mass from the positive X-axis. Then the equation of motion is simply

$$\ddot{\theta} + \cos\theta = 0 \qquad (28)$$

and the reference solutions X^* and Y^* are given by

$$X^* = \cos\theta(t) \qquad (29.a)$$

$$Y^* = \sin\theta(t) \qquad (29.b)$$

If the energy constraint control is applied, the state equation becomes

$$\ddot{\theta} = -\cos\theta - 2\rho\psi\dot{\theta} \qquad (30)$$

where

$$\psi = \frac{\dot{\theta}^2 - \dot{\theta}_0^2}{2} + g\sin\theta \qquad (31)$$

The gain ρ in (30) is chosen experimentally for smallest energy constraint violation.

Fig 4 shows geometric constraint violations Φ. In the figure the cases where independent coordinates are chosen are not compared, since the geometric constraints are inherently satisfied in these cases. Fig 4 shows that the geometric constraint controls, in either Baumgarte's CVSM or the new CVSGF, make the geometric constraint violations stable. Note that the case of no constraint control is divided by 10 for comparison in the figure. That is, the actual constraint violation is 10 times larger than the one in the figure. Fig 5 compares energy constraint violations ψ. Note that some time histories are divided by corresponding numbers for comparison in the figure. It shows that Baumgarte's geometric constraint control yields the largest energy constraint violation without energy constraint control. Even when an independent coordinate is chosen, the energy constraint violation is diverging without energy constraint

control. Finally, in Fig 6 the time domain errors in X are compared. The reference solution for X* is obtained by using RK-4 and h = 0.00001 to integrate (28). Fig 6 shows that Baumgarte's CVSM without energy constraint control yields the largest time domain errors in X, even worse than the case where no constraint controls are applied. It can also be noticed that even in the case where an independent coordinate is chosen, the energy constraint control is essential for suppressing errors in the state variable.

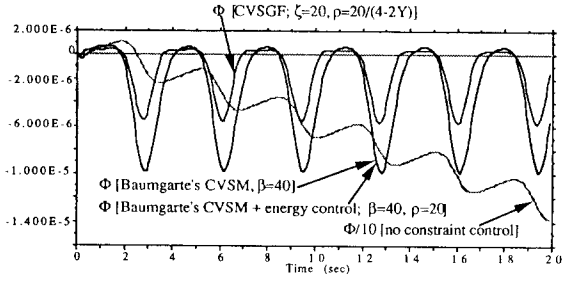

Fig 4. Example 1 [AB-3, h=0.01] : geometric constraint viol

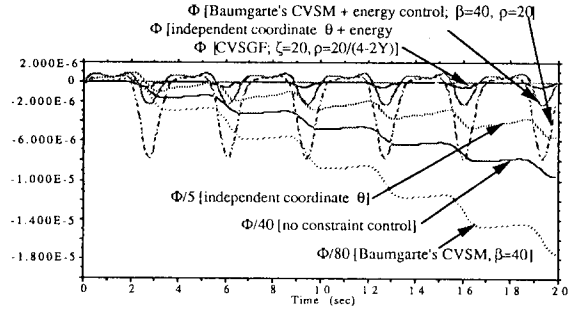

Fig 5. Example 1 [AB-3, h=0.01] : energy constraint viol

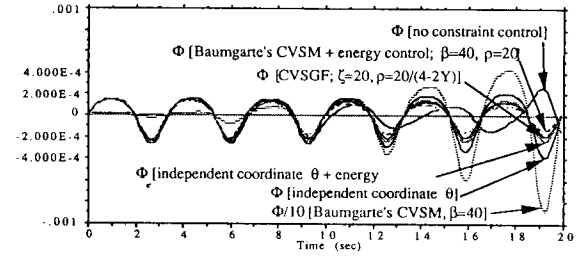

Fig 6. Example 1 [AB-3, h=0.01] : errors in the state varia

Conclusion

In the numerical simulation of constrained dynamic systems, geometric constraint control without energy constraint control worsens the time domain errors in state variables. The new constraint control in (23) is very effective and easy to implement in controlling errors of either geometric constraints or an energy constraint. Energy constraint control can be easily applied for more accurate simulation even when independent coordinates are chosen.

References

[1] Greenwood, D. T., Principles of Dynamics, Prentice-Hall, 1988.

[2] Greenwood, D. T., Classical Dynamics, Prentice-Hall, 1977.

[3] Gear, C. W.,"The Simultaneous Numerical Solution of Differential-Algebraic Equations," IEEE Trans. Circuit Theory, TC-18, 1971, pp. 89-95.

[4] Petzold, L. R.,"Differential/ Algebraic Equations Are Not ODE's," SIAM Journal on Scientific and Statistical Computing, Vol. 3, No. 3, 1982, pp. 367-384.

[5] Gear, C. W.,"Differential-Algebraic Equations," Computer Aided Analysis and Optimization of Mechanical System Dynamics, ed., E. J. Haug, NATO ASI Series, Series F, Vol. 9, Springer-Verlag, Heidelberg, 1984, pp. 323-334.

[6] Gear, C. W. and Leimkuhler, B.,"Automatic Integration of Euler-Lagrange Equations with Constraints," Journal of Computational and Applied Mathematics, Vol 12 & 13, 1985, pp. 77-90.

[7] Chace, M. A. and Smith, D. A.,"DAMN-A Digital Computer Program for the Dynamic Analysis of Generalized Mechanical Systems," SAE Paper 710244, Jan. 1971.

[8] Nikravesh, P. E.,"Some Methods for Dynamic Analysis of Constrained Mechanical Systems: A Survey," Computer Aided Analysis and Optimization of Mechanical System Dynamics, ed., E. J. Haug, Springer-Verlag, Heidelberg, 1984, pp. 351-368.

[9] Baumgarte, J.,"Stabilization of Constraints and Integrals of Motion in Dynamical Systems," Computer Methods in Applied Mechanics and Engineering, 1972, pp. 1-16.

[10] Housner, A., Analog and Analog/Hybrid Computer Programming, Prentice-Hall, 1971.

[11] Turner, R. M., "On the Reduction of Error in Certain Analog Computer Calculations by the Use of Constraint Equations," Proceedings SJCC San Francisco, 1960.

[12] Fogarty, L. E. and Howe, R. M.,"Axis Systems for Analog and Digital Computation of Space and Reentry Trajectories," Application Report, Applied Dynamics, Inc., Ann Arbor, Michigan, September, 1963.

[13] Fogarty, L. E. and Howe, R. M.,"Space Trajectory Computations at The University of Michigan," Simulation, Vol. 6, No. 4, 1966, pp. 220-226.